Astragaloside IV ameliorates endoplasmic reticulum stress-induced apoptosis of Aβ25-35-treated PC12 cells by inhibiting the p38 MAPK signaling pathway

YUHONG MA and LI XIONG

Department of Diagnostics, Wannan Medical College, Wuhu, Anhui 241001, P.R. China

Received January 29, 2018; Accepted September 10, 2018

DOI: 10.3892/mmr.2019.9855

Abstract. Endoplasmic reticulum stress (ERS) serves a vital role in the pathological development of Alzheimer's disease (AD). ERS can promote programmed cell death (apoptosis) during AD; however, the specific molecular mechanisms that lead to ERS remain unclear. It is very important that a drug for the treatment of AD is identified. Our previous studies indicated that astragaloside IV (AST IV) has anti-inflammatory effects and helps cells resist oxidative stress. In the present study, western blotting and reverse transcription semi-quantitative polymerase chain reaction were used to detect protein and mRNA expression levels, flow cytometry was used to measure intracellular reactive oxygen species (ROS) levels, and superoxide dismutase (SOD) and malondialdehyde (MDA) activity was detected using commercially available kits. The results demonstrated that SOD activity was decreased, and MDA content, ROS levels, and the expression levels of p38 mitogen-activated protein kinase (MAPK) and ERS-associated proteins, including binding immunoglobulin protein/glucose-regulated protein and growth arrest- and DNA damage -inducible gene 153/C/EBP homologous protein, were increased in amyloid β $(Aβ)_{25-35}$-treated PC12 cells. Furthermore, to investigate the role of p38 MAPK and the effects of AST IV in an *in vitro* model of AD, SB203580, a p38 MAPK signaling pathway inhibitor, and AST IV were administered to $Aβ_{25-35}$-treated PC12 cells. The results revealed that AST IV protected the cells against AD. This effect may be caused by decreases in ROS levels, which may inhibit the p38 MAPK signaling pathway and thereby suppress ERS in $Aβ_{25-35}$-treated PC12 cells.

Correspondence to: Dr Yuhong Ma, Department of Diagnostics, Wannan Medical College, 22 West Wenchang Road, Wuhu, Anhui 241001, P.R. China
E-mail: mayh1978@126.com

Key words: astragaloside IV, Alzheimer's disease, reactive oxygen species, p38 mitogen-activated protein kinase, phosphorylated-p38 mitogen-activated protein kinase, growth arrest- and DNA damage-inducible gene 153/C/EBP homologous protein, binding immunoglobulin protein/glucose-regulated protein 78

Introduction

Alzheimer's disease (AD) is a common neurodegenerative disorder in the elderly population worldwide (1). Various biologically plausible explanations for the pathogenesis of AD have been proposed. These explanations include the endoplasmic reticulum stress (ERS) hypothesis, the genetic factor hypothesis, the cholinergic hypothesis and the lack of nerve growth factor hypothesis (2,3) Among these hypotheses, the ERS hypothesis appears to be the most probable as ERS is induced by oxidative stress; ERS occurs in the earliest stages of AD pathogenesis (4). Numerous studies have attempted to ameliorate ERS as a therapy for AD (5-8); however, the specific molecular mechanisms that lead to ERS during the pathological progression of AD remain unknown. In the present study, these mechanisms and potential targeting approaches were investigated in an *in vitro* model of AD (6). The p38 mitogen-activated protein kinase (p38 MAPK) signaling pathway is mainly involved in ERS (9-11); however, the molecular mechanisms underlying ERS, and the association between ERS and the p38 MAPK signaling pathway in AD require further investigation. The present study proposed that acetyl amyloid β $(Aβ)_{25-35}$ may induce oxidative stress via p38 MAPK, resulting in ERS-associated apoptosis of PC12 cells.

Therapeutic agents for the treatment of AD have numerous side effects, including increased likelihood of bone fractures and heart failure (12). Thus, it is important to find an alternative drug with minimal side effects. Astragaloside IV (AST IV), a monomer extracted from *Astragalus*, is a herbal remedy widely used for the treatment of diabetes and diabetic nephropathy, and inhibits the effects of oxidative stress (7-9). Li *et al* (10) reported that AST IV treatment increased peroxisome proliferator-activated receptor γ and β-secretase 1 expression, and reduced neuritic plaque formation and Aβ levels in the brains of APP/PS1 mice. The present study hypothesized that AST IV, as a p38 MAPK antagonist, may suppress ERS by downregulating p38 MAPK expression and Aβ levels in patients with AD. To evaluate this hypothesis, $Aβ_{25-35}$ was applied to PC12 cells to mimic an *in vitro* models of AD; AST IV was applied to assess whether p38 MAPK expression

is affected and whether it may be a safe and effective drug for treating patients with AD.

Materials and methods

Cell culture and administration. PC12 cells (Cell Bank of Type Culture Collection of the Chinese Academy of Sciences, Shanghai, China) were incubated in Dulbecco's modified Eagle's medium (DMEM; HyClone; GE Healthcare Life Sciences, Shanghai, China) supplemented with 10% fetal bovine serum (FBS; HyClone; GE Healthcare Life Sciences), 100 U/ml penicillin and 100 μg/ml streptomycin at 37˚C in a humidified atmosphere of 5% CO_2. An *in vitro* model of AD was established by incubating the cells with 20 mM $A\beta_{25-35}$ at 37˚C for 24 h to induce PC12 cell damage. The cells were treated with AST IV (50, 100 and 200 μM; ShangHai YuanYe Biotechnology Co., Ltd., Shanghai, China) or SB203580 (20 μM; Sigma-Aldrich; Merck KGaA, Darmstadt, Germany) at 37˚C for 24 h after the model was established. Untreated cells served as the control.

Superoxide dismutase (SOD) and malondialdehyde (MDA) assay. Following treatment with AST IV or SB203580, the cells were centrifuged at 111 x g for 5 min at room temperature and the supernatants from all groups were collected. SOD (cat. no. A001-1) and MDA (cat. no. A003-1) (both from Nanjing Jiancheng Bioengineering Institute, Nanjing, China) assays were performed according to the manufacturer's protocols. Optical densities were measured at 570 nm using an Epoch microplate reader (BioTek Instruments, Inc., Winooski, VT, USA).

Reactive oxygen species (ROS) assay. Carboxy-2', 7'-dichlorodihydrofluorescein diacetate (H_2DCFDA; Sigma-Aldrich; Merck KGaA) was used to detect intracellular ROS production. Following the drug incubations, the cells were incubated with 20 μM H_2DCFDA at 37˚C for 30 min in the dark. Then the cells were detached using 0.5 g/l trypsin at 37˚C for 2 min and washed with PBS three times. Trypsin was deactivated with PBS supplemented with 3% FBS, and cells were centrifuged (111 x g for 5 min at room temperature). The levels of ROS in PC12 cells was measured by a FACScan flow cytometer and the data were processed with FlowJo software 7.6 (FlowJo LLC, Ashland, OR, USA).

RNA extraction and reverse transcription semi-quantitative polymerase chain reaction (RT-sqPCR). TRIzol (Invitrogen; Thermo Fisher Scientific, Inc., Waltham, MA, USA) was used to extract total RNA from cells and a First-Strand cDNA Synthesis kit (Thermo Fisher Scientific, Inc.) was utilized to reverse transcribe mRNA according to the manufacturer's protocols. cDNA was used as the template for sqPCR amplification using oligo primers; the internal control for the analysis was GAPDH. The primer sequences of the binding immunoglobulin protein (BIP)/glucose-regulated protein 78 (GRP78), growth arrest- and DNA damage-inducible gene 153 (GADD153)/C/EBP homologous protein (CHOP) and caspase-3 genes (Sangon Biotech Co., Ltd., Shanghai, China) are presented in Table I. PCR analysis was performed on the BIO-RAD MyCycle thermocycler (Bio-Rad Laboratories, Inc., Hercules, CA, USA) with a total reaction volume of 12 μl in each well, which contained 3 μl of PCR Master Mix (2X) (Thermo Fisher Scientific, Inc.), 3 μl of cDNA, 1 μM forward primers, 1 μM reverse primers and 2 μl of DEPC ddH_2O. Each group was assessed in triplicate. The thermocycling conditions for PCR were as follows: Initial heating at 95˚C for 10 min, 35 cycles of denaturation at 94˚C for 30 sec, annealing at 58˚C for 1 min and extension at 72˚C for 1 min, and final extension at 72˚C for 7 min. The PCR products were separated on a 1.5% agarose gel and photographed using a gel imaging system (SIM International Group Co., Ltd., Newark, DE, USA). ImageJ Software 1.49 (National Institutes of Health, Bethesda, MD, USA) was used to quantify the grey values of the DNA bands.

Western blot analysis. Following treatment, PC12 cells were lysed using western lysis buffer (Beyotime Institute of Biotechnology, Haimen, China) containing 1% PMSF on ice for 30 min for protein extraction. Protein concentration was determined using a BCA Protein Quantification kit (cat. no. P0010; Beyotime Institute of Biotechnology, Beijing, China). Equal amount of protein (10 μg) was separated on an 8 or 10% SDS-PAGE gel and the proteins were transferred to a polyvinylidene difluoride membrane (Merck KGaA). Subsequently, the membrane was blocked with 5% non-fat milk for 1 h at room temperature, and incubated with anti-p38 MAPK (1:500; cat. no. ab32142; Abcam, Cambridge, UK), anti-phosphorylated (p)-p38 MAPK (1:500; cat. no. 4511P), anti-BIP/GRP78 (1:500; cat. no. 3183S) (both from Cell Signaling Technology, Inc., Danvers, MA, USA), anti-GADD153/CHOP (1:500; cat. no. sc-575; Santa Cruz Biotechnology, Inc., USA), anti-caspase-3 (1:500; cat. no. 9665S; Cell Signaling Technology, Inc.) and anti-β-actin (1:500; cat. no. A1978; Sigma-Aldrich; Merck KGaA) primary antibodies overnight at 4˚C. Then, the membrane was incubated with horseradish peroxidase-conjugated goat anti-mouse (1:2,000; cat. no. ZB2305) or goat anti-rabbit secondary antibodies (1:2,000; cat. no. ZB2301) (both from OriGene Technologies, Inc., Beijing, China) at room temperature for 1 h. An enhanced chemiluminescence advanced western blotting detection kit (Pierce; Thermo Fisher Scientific, Inc.) was used to visualize the protein bands, which were then developed on an X-ray film. Quantity One software 4.6.6 (Bio-Rad Laboratories, Inc.) was used to quantify the grey values of the protein bands.

Statistical analysis. All experiments were repeated three times. All quantified results were expressed as the mean ± standard error of the mean. Statistical analyses were performed with SPSS 17.0 software (SPSS, Inc., Chicago, IL, USA). One-way analysis of variance followed by Student-Newman-Keuls post hoc test was used to compare the mean values of the results from each group. $P<0.05$ was considered to indicate a statistically significant difference.

Results

Oxidative stress is induced by $A\beta_{25-35}$ in PC12 cells. To assess whether treatment with 20 mM $A\beta_{25-35}$ for 24 h induced oxidative stress in PC12 cells, SOD activity, MDA content and intercellular ROS levels were assessed. SOD activity

Table I. Primer sequences for reverse transcription-quantitative polymerase chain reaction.

Gene	Forward (5'-3')	Reverse (5'-3')	Length (bp)
BIP	CCTCAGAGTGGAGTTGAAAATGC	CCCCAAGACACGTGAGCAA	82
CHOP	GGAAGTGCATCTTCATACACCACC	TGACTGGAATCTGGAGAGCGCGAGGG	316
Caspase-3	CTGGACTGCGGTATTGAG	GGGTGCGGTAGAGTAAGC	101
β-actin	AGGGAAATCGTGCGTGACAT	AACCGCTCATTGCCGATAGT	148

BIP, binding immunoglobulin protein; CHOP, C/EBP homologous protein.

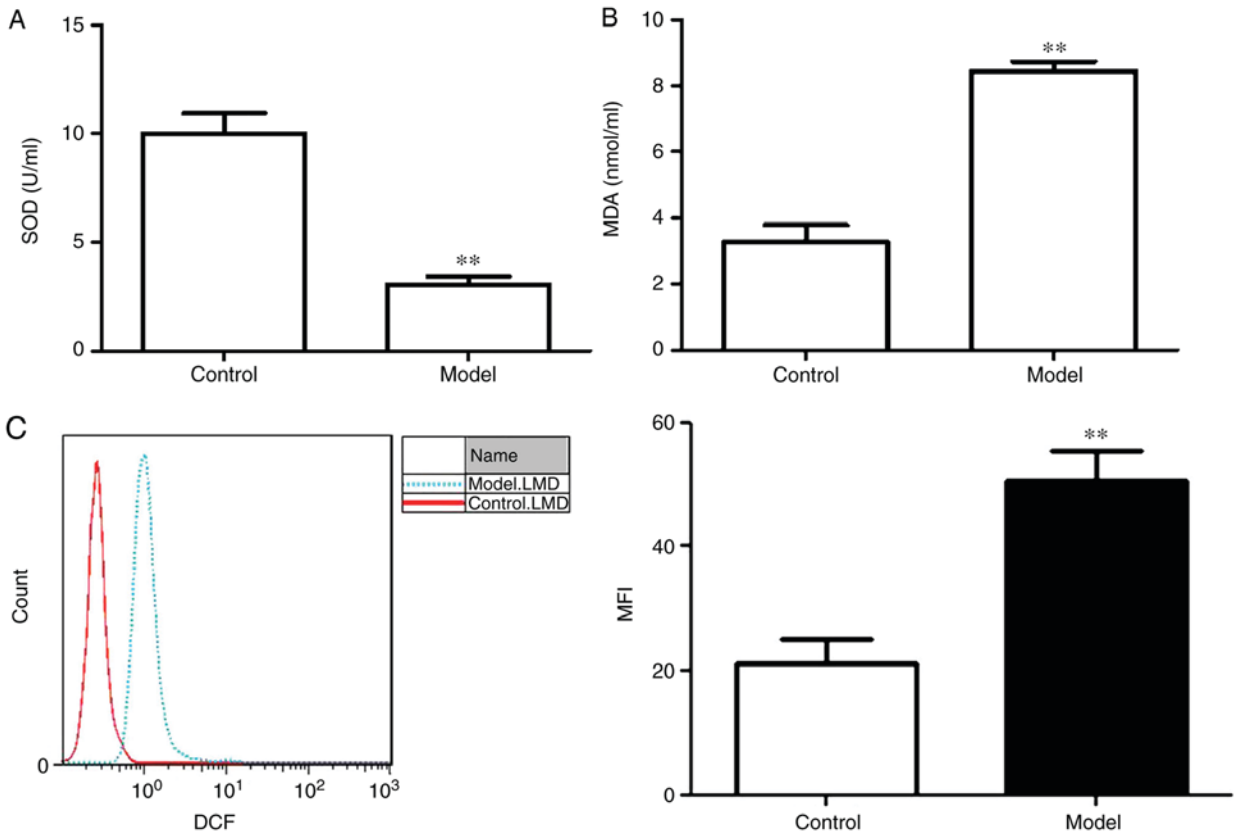

Figure 1. Oxidative stress is induced by amyloid $\beta_{25\text{-}35}$ in PC12 cells. (A) SOD activity and (B) MDA content were measured from the supernatants of the control and model groups. (C) FACS was performed to assess intercellular ROS levels in the control and model groups. **P<0.01 vs. Control. MDA, malondialdehyde; MFI, mean fluorescence intensity; ROS, reactive oxygen species; SOD, superoxide dismutase.

was significantly lower and MDA content was significantly increased in the model group compared with the control group (P<0.01; Fig. 1A and B). Similarly, the mean fluorescence intensity of ROS in the model group was significantly higher compared with the control group (Fig. 1C).

The p38 MAPK signaling pathway is activated in $A\beta_{25\text{-}35}$-treated PC12 cells. The results of the present study demonstrated that the expression of p38 MAPK protein was significantly increased in the model group compared with the control group (P<0.01; Fig. 2). The results suggested that $A\beta_{25\text{-}35}$ activated the p38 signaling pathway.

$A\beta_{25\text{-}35}$ may contribute to the ERS-induced apoptosis of PC12 cells. The expression levels of BIP/GRP78 and GADD153/CHOP, two important ERS-associated proteins, and caspase-3, a terminal apoptotic indicator (13), were examined in $A\beta_{25\text{-}35}$-treated PC12 cells. As presented in Fig. 3A and B, the mRNA and protein expression levels of BIP/GRP78, GADD153/CHOP and caspase-3 in the model group were significantly upregulated compared with the control group (P<0.01).

AST IV inhibits oxidative stress in $A\beta_{25\text{-}35}$-treated PC12 cells in a concentration-dependent manner. As presented in Fig. 4, $A\beta_{25\text{-}35}$ significantly decreased the activity of SOD, and increased the content of MDA and the level of ROS in PC12 cells compared with the control; however, treatment with 50, 100 and 200 μM AST IV significantly elevated SOD activity, and reduced MDA content and ROS levels in a dose-dependent manner (P<0.01; Fig. 4A-C). The middle dose of AST IV (100 μM) was used for subsequent experiments.

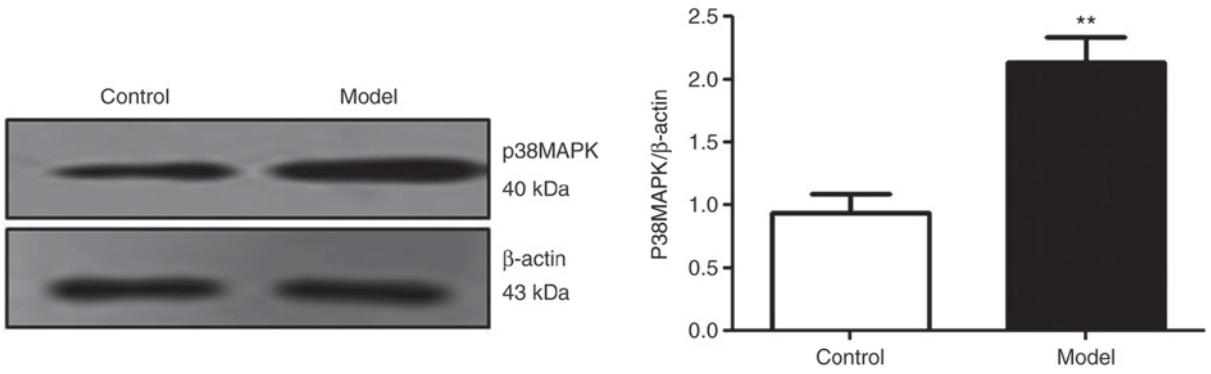

Figure 2. p38 MAPK is activated in amyloid β_{25-35}-treated PC12 cells. **P<0.01 vs. Control. MAPK, mitogen-activated protein kinase signaling pathway.

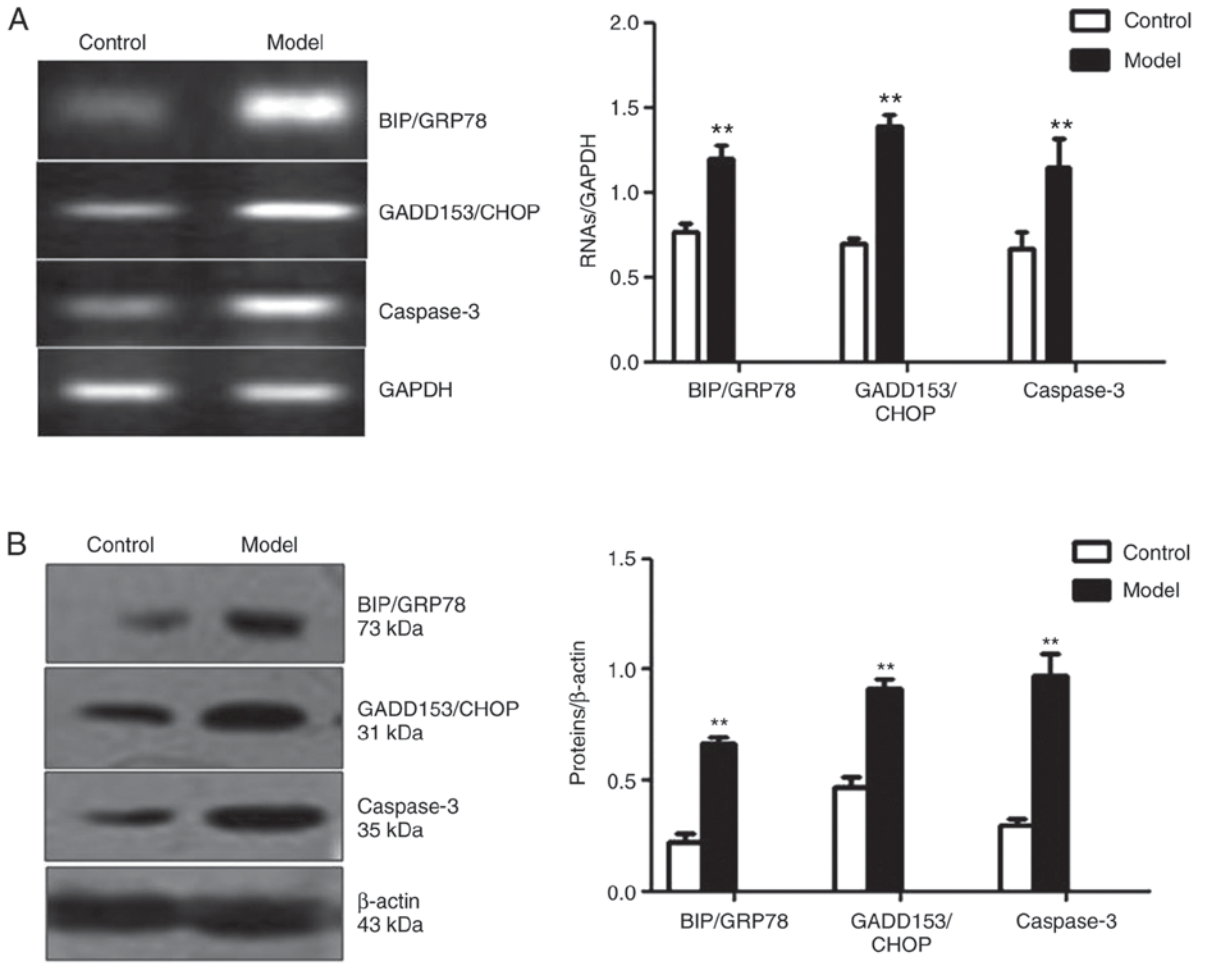

Figure 3. Amyloid β_{25-35} contributes to endoplasmic reticulum stress-induced apoptosis of PC12 cells. (A) Reverse transcription and (B) western blot analyses for BIP/GRP78, GADD153/CHOP and caspase-3 proteins in PC12 cells from the control and model groups. **P<0.01 vs. Control. BIP/GRP78, binding immunoglobulin protein/glucose-regulated protein 78; GADD153/CHOP, growth arrest- and DNA damage-inducible gene 153/C/EBP homologous protein.

AST IV ameliorates Aβ$_{25-35}$-induced ERS in PC12 cells via the p38 MAPK signaling pathway. The present study reported that Aβ$_{25-35}$ induced p38 MAPK expression in PC12 cells. SB203580, a specific inhibitor of p38 MAPK, was incubated with PC12 cells to further investigate whether oxidative stress induced ERS in PC12 cells via the p38 MAPK signaling pathway. The results revealed that SB203580 treatment significantly increased SOD activity, and significantly decreased MDA content and intercellular ROS levels compared with the model group (P<0.01, Fig. 5A-C). In addition, it was observed that p-p38 MAPK protein expression was significantly decreased in the SB203580 group compared with in the model group (P<0.01; Fig. 5D). Furthermore, SB203580 significantly reduced the expression levels of BIP/GRP78, GADD153/CHOP and caspase-3 compared with the model group (P<0.01; Fig. 5E and F). AST IV (100 μM) significantly ameliorated the effects induced by Aβ$_{25-35}$, potentially by alleviating oxidative stress (P<0.01; Fig. 5A-C); a significantly

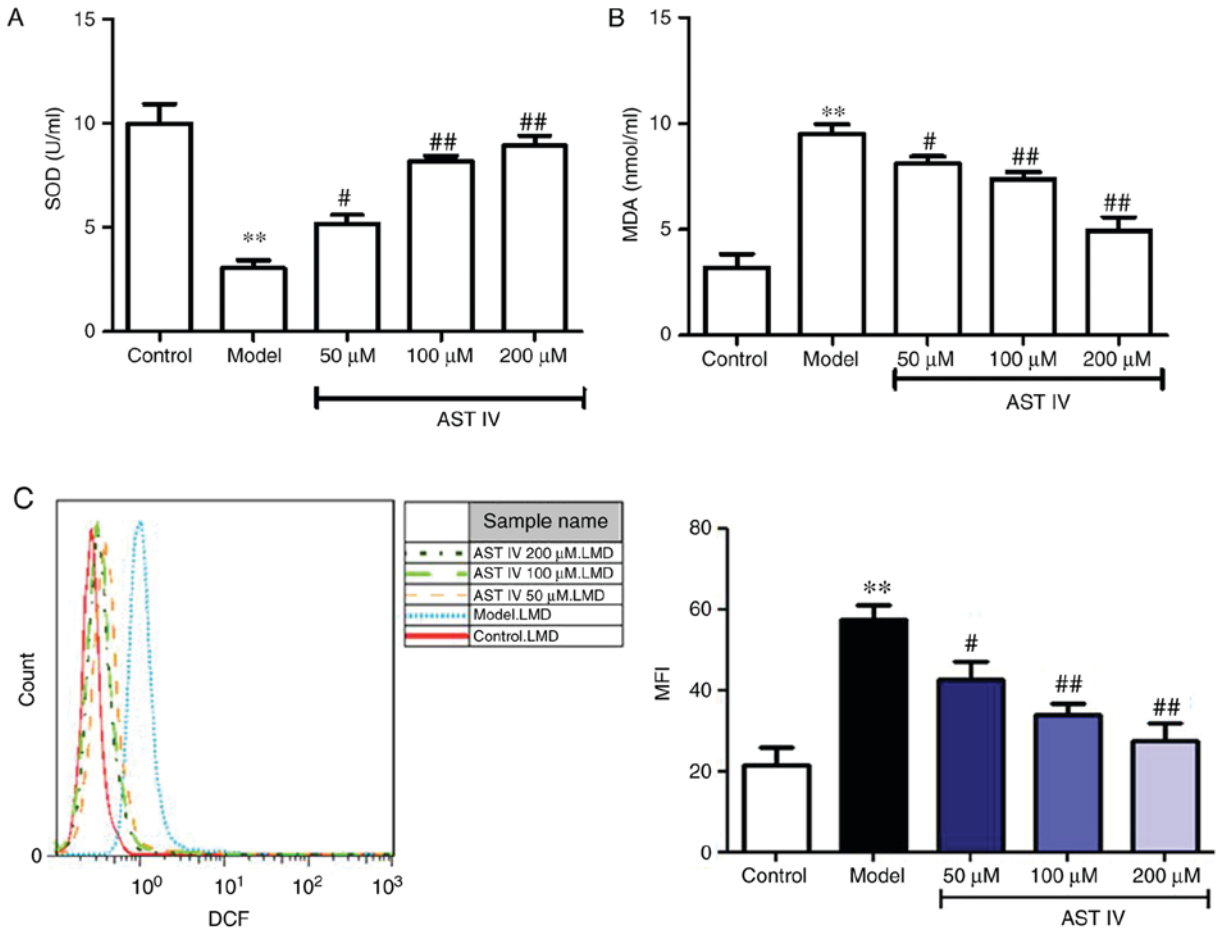

Figure 4. AST IV alleviates oxidative stress in amyloid β_{25-35}-treated PC12 cells. (A) SOD activity and (B) MDA content were measured from the supernatants of the control, model, 50, 100 and 200 μM AST IV groups. (C) FACS was performed to assess intercellular ROS levels in the control, model, 50, 100 and 200 μM AST IV groups. **P<0.01 vs. Control; $^{\#}$P<0.05, $^{\#\#}$P<0.01 vs. Model. AST IV, astragaloside IV; MDA, malondialdehyde; SOD, superoxide dismutase.

reduced p-p38 MAPK ratio and decreased caspase-3 expression in PC12 cells was also reported (P<0.05; Fig. 5D-F).

Discussion

ERS serves a vital role in the earliest stages of AD pathogenesis (6). Recent studies have demonstrated that the toxic peptide, Aβ, induces ERS and then activates the unfolded protein response (8,13). It has been reported that ERS is involved in the cleavage of Aβ protein precursor, thus promoting the production of Aβ and facilitating the development of AD (14-16). The results of the present study revealed that treatment with 20 mM $A\beta_{25-35}$ for 24 h contributed to the unbalancing of the redox state by reducing SOD activity, and increasing MDA content and ROS accumulation in PC12 cells, consistent with previous studies (17,18). The results also indicated that the expression levels of ERS-specific proteins, BIP/GRP78 and GADD153/CHOP, were increased in PC12 cells in response to $A\beta_{25-35}$ treatment (19). Under particular conditions, including lipid accumulation, glucose deprivation or oxidative stress, ER homeostasis is dysregulated, which induces the accumulation of misfolded proteins within the ER lumen (20,21). Consequently, cells are unable to respond to unfolded proteins and they succumb to apoptosis (15,22). It was previously reported that oxidative stress activated antiapoptotic ER chaperone proteins, including BIP/GRP78, but severe ERS activated proapoptotic ER chaperone proteins, including GADD153/CHOP (23). The identification of these unfolded protein response markers indicated an association between cell death and ERS. Apoptosis is known as a possible cell death mechanism in age-associated diseases, and is regulated by complex signaling pathways and enzymatic cascades. Caspase-3 is a terminal indicator of apoptosis and cytokine processing (24); the present study indicated that the expression levels of Caspase3 mRNA and proteins were upregulated as previously reported.

Jian *et al* reported that treatment with SB203580, a p38 MAPK inhibitor, inhibited ROS generation in myocardial cells, thus protecting the cells from doxorubicin-induced apoptosis (25). The results of the present study also demonstrated that treatment with 20 mM $A\beta_{25-35}$ induced p38 MAPK activation, consistent with recent studies (26,27). To investigate the role of p38 MAPK in an *in vitro* model of AD, SB203580 was administered. The results revealed that SB203580 administration could decrease ROS levels, ERS and caspase-3 expression in $A\beta_{25-35}$-treated PC12 cells, which were consistent with previous studies (28-30). The present study indicated that AST IV exhibited similar effects to SB203580; it is possible that the mechanism of AST IV is associated with the enhancement of SOD activity, which is an important enzyme in cellular oxidative injury (31), decreased MDA content and inhibition of ROS aggregation. It

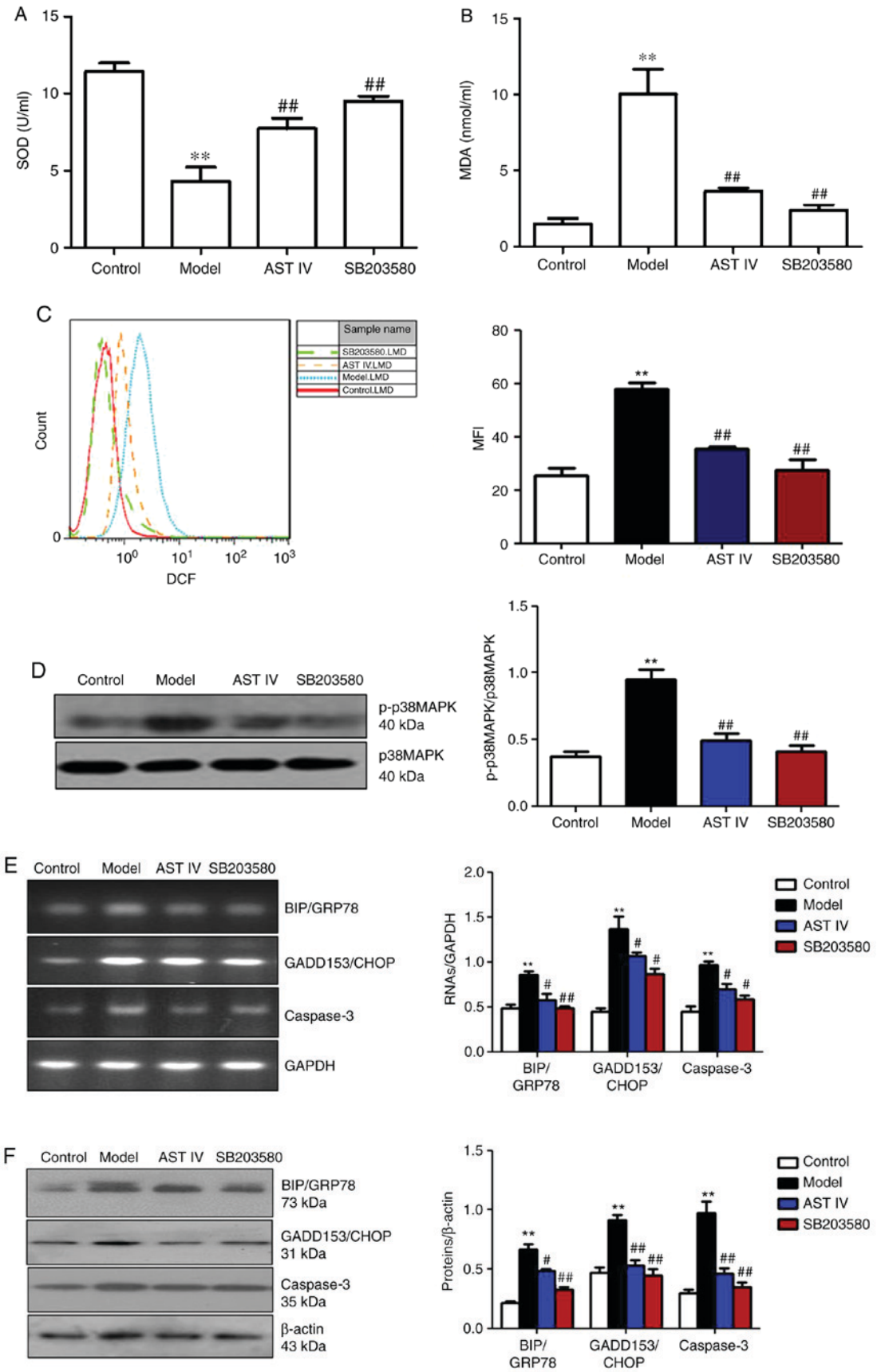

Figure 5. AST IV (100 μM) and SB203580 ameliorate apoptosis in PC12 cells induced by amyloid $\beta_{25\text{-}35}$ via p38 MAPK. (A) SOD activity and (B) MDA content were measured from the supernatants from the control, model, AST IV and SB203580 groups. (C) FACS was performed to assess intercellular ROS levels in the control, model, AST IV and SB203580 groups. (D) Western blot analyses of p38 MAPK and p-p38 MAPK. (E and F) Reverse transcription semi-quantitative polymerase chain reaction and western blot analyses of BIP/GRP78, GADD153/CHOP and caspase-3 were performed of the control, model, AST IV and SB203580 groups. **P<0.01 vs. Control; $^{\#}$P<0.05, $^{\#\#}$P<0.01 vs. Model. AST IV, astragaloside IV; BIP/GRP78, binding immunoglobulin protein/glucose-regulated protein 78; GADD153/CHOP, growth arrest- and DNA damage-inducible gene 153/C/EBP homologous protein; MAPK, mitogen-activated protein kinase; MDA, malondialdehyde; SOD, superoxide dismutase.

was suggested that the p38 MAPK signaling pathway serves a role in the pathogenesis of AD in $A\beta_{25-35}$-treated PC12 cells. By suppressing the p38 MAPK signaling pathway and treating cells with AST IV, the protein expression of BIP/GRP7, GADD153/CHOP and caspase-3 may be downregulated.

It remains unknown whether other oxidative stress-associated signaling pathways are involved in ERS, which is a limitation of our study. Further investigation is required to determine the molecular mechanism underlying the pharmacological effects of AST IV in patients with AD and to understand the role of other signaling pathways. In conclusion, these data suggested that PC12 cells treated with 20 mM $A\beta_{25-35}$ for 24 h induced ERS-associated apoptosis, which may be partly due to oxidative stress, as ERS is induced by activating the p38 MAPK signaling pathway (32). The results of the present study suggest that AST IV may possess therapeutic potential in the treatment of AD.

Acknowledgements

Not applicable.

Funding

This study was supported by the Natural Science Foundation of Anhui (grant no. 1508085SMH236) and the Introduction and Cultivation Project of Leading Talents in Universities and Colleges of Anhui Province-Visiting Scholar (grant no. gxfxZD2016162).

Availability of data and materials

The datasets used and/or analyzed during the current study are available from the corresponding author on reasonable request.

Authors' contributions

LX performed the experiments, including cell culture, western blot analysis and polymerase chain reaction. YM made substantial contributions to the conception and design of the study, and was involved in drafting the manuscript and revising it critically for important intellectual content. All authors read and approved the final manuscript.

Ethics approval and consent to participate

Not applicable.

Patient consent for publication

Not applicable.

Competing interests

The authors declare that they have no competing interests.

References

1. Ide K, Matsuoka N and Kawakami K: Is the use of proton-pump inhibitors a risk factor for Alzheimer's disease? Molecular mechanisms and clinical implications. Curr Med Chem 25: 2166-2174, 2018.
2. Lista S, Khachaturian ZS, Rujescu D, Garaci F, Dubois B and Hampel H: Application of systems theory in longitudinal studies on the origin and progression of Alzheimer's disease. Methods Mol Biol 1303: 49-67, 2016.
3. Ellis B, Hye A and Snowden SG: Metabolic modifications in human biofluids suggest the involvement of sphingolipid, antioxidant, and glutamate metabolism in Alzheimer's disease pathogenesis. J Alzheimers Dis 46: 313-327, 2015.
4. Liu H, Zhang X, Zhang S, Huang H, Wu J, Wang Y, Yuan L, Liu C, Zeng X, Cheng X, *et al*: Oxidative stress mediates microcystin-LR-induced endoplasmic reticulum stress and autophagy in KK-1 cells and C57BL/6 mice ovaries. Front Physiol 9: 1058, 2018.
5. Adzic M, Mitic M and Radojcic M: Mitochondrial estrogen receptors as a vulnerability factor of chronic stress and mediator of fluoxetine treatment in female and male rat hippocampus. Brain Res 1671: 77-84, 2017.
6. Chen W, Chan Y, Wan W, Li Y and Zhang C: $A\beta_{1-42}$ induces cell damage via RAGE-dependent endoplasmic reticulum stress in bEnd.3 cells. Exp Cell Res 362: 83-89, 2018.
7. Fraga FJ, Mamani GQ, Johns E, Tavares G, Falk TH and Phillips NA: Early diagnosis of mild cognitive impairment and Alzheimer's with event-related potentials and event-related desynchronization in N-back working memory tasks. Comput Methods Programs Biomed 164: 1-13, 2018.
8. Song X, Liu B, Cui L, Zhou B, Liu L, Liu W, Yao G, Xia M, Hayashi T, Hattori S, *et al*: Estrogen receptors are involved in the neuroprotective effect of silibinin in $A\beta_{1-42}$-treated rats. Neurochem Res 43: 796-805, 2018.
9. Kheiri G, Dolatshahi M, Rahmani F and Rezaei N: Role of p38/MAPKs in Alzheimer's disease: Implications for amyloid beta toxicity targeted therapy. Rev Neurosci, 2018.
10. Li J, Ma X, Wang Y, Chen C, Hu M, Wang L, Fu J, Shi G, Zhang D and Zhang T: Methyl salicylate lactoside protects neurons ameliorating cognitive disorder through inhibiting amyloid beta-induced neuroinflammatory response in Alzheimer's disease. Front Aging Neurosci 10: 85, 2018.
11. Melone MAB, Dato C, Paladino S, Coppola C, Trebini C, Giordana MT and Perrone L: Verapamil inhibits Ser202/Thr205 phosphorylation of Tau by blocking TXNIP/ROS/p38 MAPK pathway. Pharm Res 35: 44, 2018.
12. Wong BL, Rybalsky I, Shellenbarger KC, Tian C, McMahon MA, Rutter MM, Sawnani H and Jefferies JL: Long-term outcome of interdisciplinary management of patients with duchenne muscular dystrophy receiving daily glucocorticoid treatment. J Pediatr 182: 296-303.e1, 2017.
13. Shen H, Pan XD, Zhang J, Zeng YQ, Zhou M, Yang LM, Ye B, Dai XM, Zhu YG and Chen XC: Endoplasmic reticulum stress induces the early appearance of pro-apoptotic and anti-apoptotic proteins in neurons of five familial Alzheimer's disease mice. Chin Med J (Engl) 129: 2845-2852, 2016.
14. Kobylewski SE, Henderson KA, Yamada KE and Eckhert CD: Activation of the EIF2α/ATF4 and ATF6 pathways in DU-145 cells by boric acid at the concentration reported in men at the US mean boron intake. Biol Trace Elem Res 176: 278-293, 2017.
15. Liu XJ, Wei J, Shang YH, Huang HC and Lao FX: Modulation of AβPP and GSK3β by endoplasmic reticulum stress and involvement in Alzheimer's disease. J Alzheimers Dis 57: 1157-1170, 2017.
16. Lan YL, Zhao J and Li S: Update on the neuroprotective effect of estrogen receptor alpha against Alzheimer's disease. J Alzheimers Dis 43: 1137-1148, 2015.
17. Wei H, Gao Z, Zheng L, Zhang C, Liu Z, Yang Y, Teng H, Hou L, Yin Y and Zou X: Protective effects of fucoidan on Aβ25-35 and d-Gal-induced neurotoxicity in PC12 cells and d-Gal-induced cognitive dysfunction in mice. Mar Drugs 15: E77, 2017.
18. Xu P, Wang H, Li Z and Yang Z: Triptolide attenuated injury via inhibiting oxidative stress in Amyloid-Beta25-35-treated differentiated PC12 cells. Life Sci 145: 19-26, 2016.
19. Zhang J, Wu J, Zeng W, Zhao Y and Zu H: Exendin-4, a glucagon-like peptide-1 receptor agonist, inhibits Aβ25-35-induced apoptosis in PC12 cells by suppressing the expression of endoplasmic reticulum stress-related proteins. Int J Clin Exp Pathol 8: 12784-12792, 2015.
20. Basseri S and Austin RC: Endoplasmic reticulum stress and lipid metabolism: Mechanisms and therapeutic potential. Biochem Res Int 2012: 841362, 2012.
21. E L, Cheng Y and Zhao X: Protective effects of high-density lipoprotein on mice cardiomyocytes induced by oxygen and glucose deprivation through Akt signaling pathway. Zhonghua Wei Zhong Bing Ji Jiu Yi Xue 30: 795-799, 2018 (In Chinese).

22. Chen M, Liu Q, Chen L, Zhang L and Gu E: Remifentanil post-conditioning ameliorates histone H3 acetylation modification in H9c2 cardiomyoblasts after hypoxia/reoxygenation via attenuating endoplasmic reticulum stress. Apoptosis 22: 662-671, 2017.
23. Yang Q, Gao H, Dong R and Wu YQ: Sequential changes of endoplasmic reticulum stress and apoptosis in myocardial fibrosis of diabetes mellitus-induced rats. Mol Med Rep 13: 5037-5044, 2016.
24. Sánchez-Rodríguez C, Cuadrado E, Riestra-Ayora J and Sanz-Fernández R: Polyphenols protect against age-associated apoptosis in female rat cochleae. Biogerontology 19: 159-169, 2018.
25. Jian CY, Ouyang HB, Xiang XH, Chen JL, Li YX, Zhou X, Wang JY, Yang Y, Zhong EY, Huang WH and Zhang HW: Naringin protects myocardial cells from doxorubicininduced apoptosis partially by inhibiting the p38MAPK pathway. Mol Med Rep 16: 9457-9463, 2017.
26. Zhou Y, Wang ZF, Li W, Hong H, Chen J, Tian Y and Liu ZY: Protective effects of microRNA-330 on amyloid β-protein production, oxidative stress, and mitochondrial dysfunction in Alzheimer's disease by targeting VAV1 via the MAPK signaling pathway. J Cell Biochem 119: 5437-5448, 2018.
27. Guo J, Chang L, Li C, Li M, Yan P, Guo Z, Wang C, Zha Q and Wang Q: SB203580 reverses memory deficits and depression-like behavior induced by microinjection of $A\beta_{1-42}$ into hippocampus of mice. Metab Brain Dis 32: 57-68, 2017.
28. Werner E, Wang H and Doetsch PW: Opposite roles for p38MAPK-driven responses and reactive oxygen species in the persistence and resolution of radiation-induced genomic instability. PLoS One 9: e108234, 2014.
29. Yang G, Yang W, Wu L and Wang R: H2S, endoplasmic reticulum stress, and apoptosis of insulin-secreting beta cells. J Biol Chem 282: 16567-16576, 2007.
30. Park JY, Kim EJ, Kwon KJ, Jung YS, Moon CH, Lee SH and Baik EJ: Neuroprotection by fructose-1,6-bisphosphate involves ROS alterations via p38 MAPK/ERK. Brain Res 1026: 295-301, 2004.
31. Sun Y, Xun L, Jin G and Shi L: Salidroside protects renal tubular epithelial cells from hypoxia/reoxygenation injury in vitro. J Pharmacol Sci 137: 170-176, 2018.
32. Pinceti E, Shults CL, Rao YS and Pak TR: Differential effects of E2 on MAPK activity in the brain and heart of aged female rats. PLoS One 11: e0160276, 2016.